Developmental Biology 334 (2009) 224–234

Contents lists available at ScienceDirect

Developmental Biology

journal homepage: www.elsevier.com/developmentalbiology

A gain of function mutation causing skeletal overgrowth in the *rapunzel* mutant

Julie Green [a], Jennifer J. Taylor [a], Anna Hindes [b], Stephen L. Johnson [b], Matthew I. Goldsmith [a,b,*]

[a] Department of Pediatrics, Washington University School of Medicine, St. Louis, MO 63110, USA
[b] Department of Genetics, Washington University School of Medicine, St. Louis, MO 63110, USA

ARTICLE INFO

Article history:
Received for publication 19 December 2008
Revised 16 July 2009
Accepted 16 July 2009
Available online 24 July 2009

Keywords:
Zebrafish
Fin
Bone
Skeleton
Growth
Overgrowth

ABSTRACT

Mechanisms that regulate the growth and form of the vertebrate skeleton are largely unknown. The zebrafish mutant *rapunzel* has heterozygous defects in bone development, resulting in skeletal overgrowth, thus identification of the genetic lesion underlying *rapunzel* might provide insight into the molecular basis of skeletogenesis. In this report, we demonstrate that the *rapunzel* mutant results from a missense mutation in the previously uncharacterized *rpz* gene. This conclusion is supported by genetic mapping, identification of a missense mutation in *rapunzel*^{c14} in a highly conserved region of the *rpz* gene, and suppression of the *rapunzel* homozygous embryonic phenotype with morpholino knockdown of *rpz*. In addition, *rpz* transcripts are identified in regions correlating with the homozygous embryonic phenotype (head, pectoral fin buds, somites and fin fold). This report provides the first gene identification for a mutation affecting segment number in the zebrafish fin and development of both the fin ray (dermal) and the axial skeleton.

Introduction

The molecular mechanisms underpinning growth and the establishment of proper size and form are largely unknown. Vertebrate morphology is inextricably related to the growth and form of the supporting skeletal structures. Identifying mutations that result in defects in bone morphology might provide insights regarding the molecular mechanisms that regulate bone shape and size.

We used the zebrafish fin and axial skeleton as a model to examine genes critical for vertebrate bone development. Fin rays are composed of multiple segments, each segment in turn comprised of two hemirays (lepidotrichia) of dermal bone in apposition, surrounding an intra-ray mesenchyme (Santamaria et al., 1992). In addition to bone, the mesenchymal compartment contains nerves, blood vessels, pigment cells and undifferentiated fibroblasts, all surrounded by a basement membrane and an overlying epithelium. Lepidotrichia are covered on both surfaces by a monolayer of bone-forming osteoblasts (scleroblasts) that form as undifferentiated mesenchymal cells in the distal portion of the intra-ray proliferate (Goldsmith et al., 2003), condense laterally along actinotrichia, differentiate, and begin secreting bone matrix (Goss, 1978; Haas, 1962). Fin growth occurs via the sequential, distal addition of new segments of bone to each fin ray (Goss and Stagg, 1957; Haas, 1962) with fin length ultimately being determined by the number and size of these individual fin ray segments (Iovine and Johnson, 2000). Zebrafish mutants have been described that affect both the number of segments (*rapunzel* and *long fin*) (Goldsmith et al., 2003; Iovine and Johnson, 2000) and the size of individual segments (*short fin*) ((Iovine and Johnson, 2000) and some molecular details of these events have been elucidated. For example, segment length is regulated in part by the function of the gap junction protein, connexin 43 (cx43) and hypomorphic alleles of the zebrafish cx43 gene result in the zebrafish *short fin* mutant (Hoptak-Solga et al., 2007; Iovine et al., 2005). To date, the molecular identity of mutations affecting segment number have not been published, nor have mutations been described that affect growth of both the fin ray and the axial skeleton.

We have cloned and characterized the zebrafish mutant *rapunzel*. Adult zebrafish display a heterozygous overgrowth phenotype of both the fin ray and the axial skeleton. In addition, *rapunzel* has a distinct, homozygous lethal embryonic phenotype (Goldsmith et al., 2003 and Fig. 1). Utilizing this embryonic phenotype, we identified a missense mutation in a previously undescribed gene (*rpz*) of unknown function. Sequence analysis demonstrated that this mutation is not a common polymorphism and morpholino knockdown of *rpz* completely suppressed the *rapunzel* embryonic phenotype, demonstrating that *rapunzel* is a gain of function allele. In addition, extensive analysis of the *rapunzel* critical region demonstrates that *rpz* founds a family of five related genes. Finally, the region of the predicted rapunzel protein containing the missense mutation is highly conserved in teleosts. Therefore *rapunzel* provides an opportunity to gain new information about the fundamental mechanisms shaping vertebrate morphology.

* Corresponding author. Department of Pediatrics, Washington University School of Medicine, 660 South Euclid Avenue, Campus Box 8208, St. Louis, MO 63110, USA. Fax: +1 314 286 2784.
E-mail address: goldsmith_m@kids.wustl.edu (M.I. Goldsmith).

0012-1606/$ – see front matter © 2009 Elsevier Inc. All rights reserved.
doi:10.1016/j.ydbio.2009.07.025

Materials and methods

Fish husbandry

Wild type fish stocks used for these studies were from the C32 (Rawls et al., 2003) and AB strains. Fish were reared at a constant temperature of 25 °C and maintained on a 14L: 10D photoperiod. Fish were fed three times daily with both micropellets (Hikari, Aquatic Eco-Systems) and brine shrimp (Biomarine, Aquafauna Biomarine).

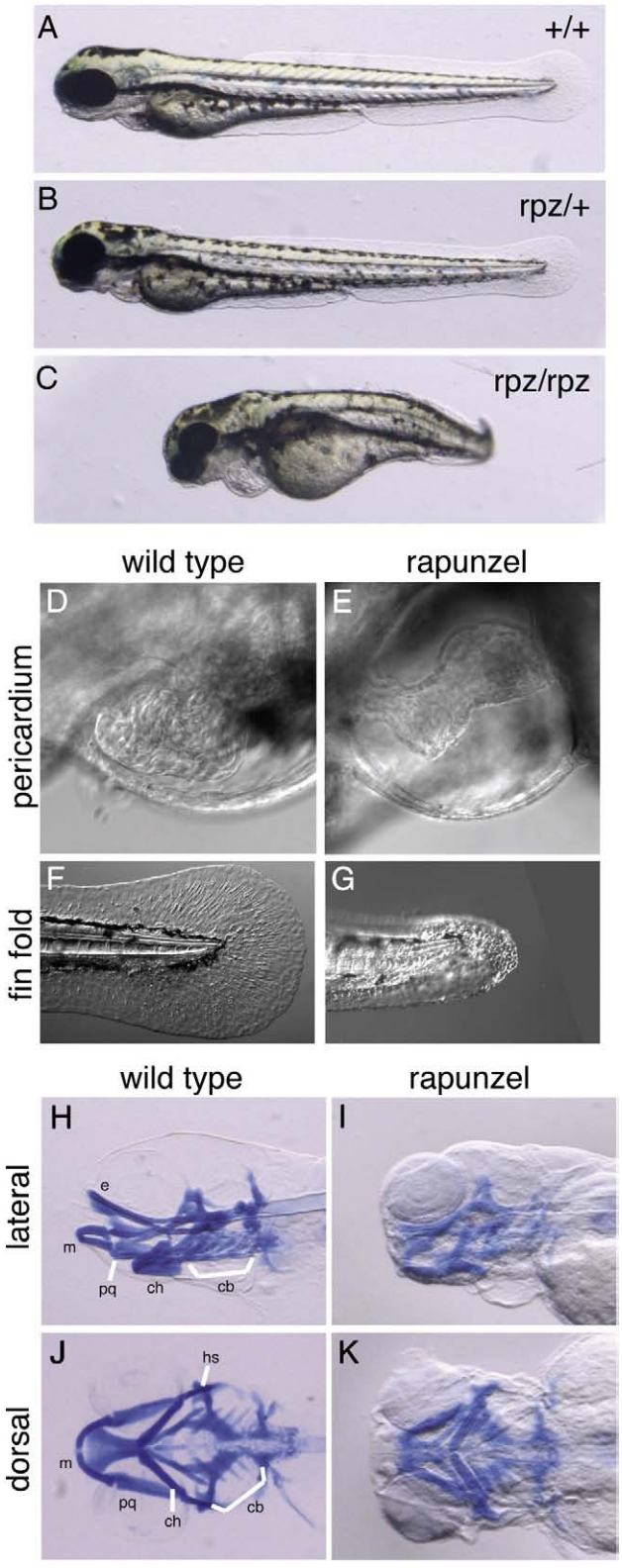

Fig. 1. Phenotype of *rapunzel* embryos. A–C. Wild type, heterozygous *rapunzel* and homozygous *rapunzel* embryos. D–G. Nomarski images of wild type (D, F) and homozygous *rapunzel* (E, G) embryos at 72 hpf demonstrating pericardial edema (E) and fin fold defects (G) in *rapunzel* mutants. H–K. Lateral (H, I) and ventral (J, K) views of whole-mount Alcian blue-stained wild type (H, J) and *rapunzel* (I, K) homozygous mutants at 96 hpf demonstrating reduced development of the craniofacial cartilages in *rapunzel* mutants. Craniofacial structures labeled as in Piotrowski et al., 1996; bh: baihyal, cb: ceratobranchial, ch: ceratohyal, e: ethmoid plate, hs: hyosymplectic, m: Meckel's cartilage, and pq: palatoquadrate.

Alizarin red and Alcian blue staining

Zebrafish were euthanized in Tricaine and fixed in 4% buffered paraformaldehyde. Embryos were then stained for developing cartilage with Alcian blue as described by Schilling et al., 1996. Embryos and larvae were stained with alizarin red as described by Walker and Kimmel, 2007. Following staining, embryos were stored in glycerol. Whole-mount specimens were imaged using a Nikon SMZ1500 stereomicroscope and photographed using Nikon ACT-1 software. Images were processed in Photoshop CS3 (Adobe).

Calcein staining

A 0.2% calcein solution was made by dissolving 2 g of calcein in 1 L of MilliQ water and adjusting the pH to ~7.0 with NaOH. Fish were immersed in calcein solution for 5–10 min and then washed with fresh system water for 10 min to clear away excess dye as previously described (Du et al., 2001). Fish were then anesthetized in 0.03% Tricaine for viewing and imaging as described above.

Sirius red staining

Wild type and *rapunzel* heterozygous fish (18 months of age) were euthanized in Tricaine, their viscera removed, and fixed over night in 4% buffered paraformaldehyde at 4 °C. Following fixation the fish were decalcified in 0.35 M EDTA, pH 7.8 for several days. Fish were then embedded in paraffin and 5 μM sections were cut on a microtome. Sections were then stained with Sirius red as previously described (Blumer et al., 2004).

MicroCT and DEXA scanning

rapunzel heterozygotes (2 months, 8 months, and 18 months) and their wild type siblings were euthanized in Tricaine and fresh frozen at −20 °C until scanned. Prior to scanning the fish were embedded in 1% agarose. Fish were scanned on a μCT40, Scanco Medical (5 kV, 177 A, 200 ms, 16 μm voxel size). Manufacturer's software (Eval v6.0) was used to calculate bone volume and apparent mineral density (calibrated to the manufacturer's hydroxyapatite [HA] mineral phantom). For DEXA scanning, total body bone mineral density (BMD) was measured by DEXA using a PIXImus scanner GE/Lunar; Madison, WI). Calibration was performed daily with a standard phantom as suggested by the manufacturer. The precision of whole-body BMD, assessed by the root mean square method is 1.34% (coefficient of variation).

Microscopy

General microscopy was performed with a Nikon SMZ1500 stereomicroscope and images captured using Nikon DXM1200F digital camera and Nikon ACT-1 software. Fluorescent images were taken using an Olympus MVX10 microscope and Olympus MicroSuite